Holographic interference electron microscopy for determining specimen magnetic structure and thickness distribution

Akira Tonomura, Tsuyoshi Matsuda, and Junji Endo
Advanced Research Laboratory, Hitachi, Ltd., Kokubunji, Tokyo 185, Japan

Tatsuo Arii
National Institute for Physiological Sciences, Okazaki, Aichi 444, Japan

Kazuhiro Mihama
Department of Applied Physics, Faculty of Engineering, Nagoya University, Chikusa-ku, Nagoya 464, Japan
(Received 21 April 1986)

A new holographic method utilizing the time-reversal operation of an electron beam has been devised to observe separately electric and magnetic phase distributions as interference electron micrographs, which had been unavailable using conventional methods. By this technique, both the magnetization and thickness distributions of three-dimensional cobalt particles have been determined.

I. INTRODUCTION

Holographic interference electron microscopy[1-3] has recently been put to practical use with the development of field-emission electron beams.[4] This technique is unique in that the thickness contour lines[5] or magnetic lines of force[6] are drawn as contour fringes on an electron micrograph. Since the fundamental principle behind this measurement lies in the interaction of an electron beam with electrostatic and magnetic vector potentials, the electron phase shift consists of two contributions, electric and magnetic. This ambiguity has often made the interpretation of interference micrographs difficult.

In magnetic domain structure observations,[7] for example, the specimen to be investigated must be uniform in thickness.[8] Otherwise, it cannot be judged whether the phase shift is due to the effect of magnetic structures or that of specimen thickness variations.

In the present investigation, a holographic method is devised for separating the electric and magnetic contributions in interference electron microscopy. This method is then used to determine the magnetization distribution inside a fine particle which is not uniform in thickness.

II. PRINCIPLE OF HOLOGRAPHIC METHOD

The phase shift ϕ of an electron beam having passed through weak electromagnetic fields is given by[9]

$$\phi=\frac{e}{\hbar}\int(m\mathbf{v}-e\mathbf{A})d\mathbf{s}\ . \tag{1}$$

Here $\hbar$, m, e, $\mathbf{v}$, and $\mathbf{A}$ are Planck's constant, electron mass, electron charge, electron velocity, and vector potential, respectively. In this equation, the line integral is performed along an electron path. The effect of the electrostatic potential (V) is contained in $m\mathbf{v}$ such that

$$\tfrac{1}{2}mv^2=\tfrac{1}{2}mv_0^2-eV\ .$$

The value of ϕ cannot be experimentally determined; instead, it is the phase difference $\Delta\phi$ between the two beams that can be observed when there is interference as shown in Fig. 1. Two coherent electron beams from a point pass through a ferromagnetic thin film at P_1 and P_2, and are brought together by a prism at another point. Then, $\Delta\phi$ is given by Eq. (1), where the line integral is carried out along a closed path determined by the two electron paths. When there are no electromagnetic fields outside the film, the phase difference between points P_1 and P_2 on the exit film surface can be given by the above $\Delta\phi$ value. It has recently become possible[6] to actually observe the $\Delta\phi$ distribution as an interference micrograph using electron holography, where a reference point P_2 is chosen as a point of free space away from the film.

If the film is uniform in thickness, $\Delta\phi$ is due completely to the magnetic structures inside the film, as given by the following equation:

$$\Delta\phi=-\frac{e}{\hbar}\oint\mathbf{A}d\mathbf{s}=-\frac{e}{\hbar}\int\mathbf{B}d\mathbf{S}\ . \tag{2}$$

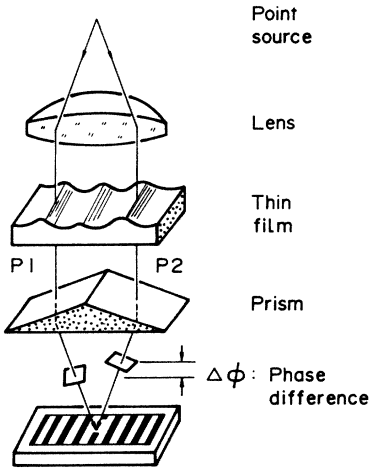

FIG. 1. Phase difference between two electron beams transmitted through a film.

In this equation, the surface integral is performed over the surface enclosed by the electron paths. It can be deduced that the contour lines of $\Delta\phi$ follow the magnetic lines of force, and that a constant magnetic flux of h/e is present between two adjacent contour lines.

When the film thickness is not uniform, on the other hand, a contribution due to the electrostatic potential is added to Eq. (2). The specimen can be regarded as a space having a higher electric potential than that of a vacuum by inner potential V_0.[10] Thus, this contribution to $\Delta\phi$ can be calculated as

$$\Delta\phi=\frac{e}{\hbar}V_0\tau=\frac{e}{\hbar}\frac{V_0 t}{v}\ . \tag{3}$$

Here τ is the transit time of an electron through a film, and is consequently given by the film thickness t divided by the electron velocity v. As a result, the contour lines of $\Delta\phi$ cannot generally be interpreted in physical terms as they can in purely electric or magnetic cases.

In order to circumvent this difficulty, the principle behind a new method, which can separate the thickness and magnetic effects, is discussed.[11] This method utilizes the differing effects on time reversal,[12] and consequently requires two holograms of the specimen. These holograms are taken from the standard specimen position and with its face turned over. In these holograms, the thickness contribution to $\Delta\phi$ is the same, but the magnetic contribution is of opposite sign.

The occurrence of the opposite sign can be simply explained using the equation for electron motion in the electric and magnetic fields, **E** and **B**:

$$m\frac{d\mathbf{v}}{dt}=-e(\mathbf{E}+\mathbf{v}\times\mathbf{B})\ . \tag{4}$$

The situation is now considered where an electron beam is incident to the specimen along the same trajectory but from the opposite direction, as illustrated in Fig. 2. This situation is equivalent to the transformation of the time reversal: $t\rightarrow -t$ and $\mathbf{v}\rightarrow -\mathbf{v}$. Thus, the equation of motion becomes

$$m\frac{d\mathbf{v}}{dt}=-e(\mathbf{E}-\mathbf{v}\times\mathbf{B})\ . \tag{5}$$

For purely electric cases ($\mathbf{B}=\mathbf{0}$), the resultant trajectory is represented exactly by the original equation (4). For a magnetic case, however, the trajectory is not the same unless the direction of magnetic field **B** is reversed ($-\mathbf{B}$).[13] These results based on the classical analysis also hold for the wave-optical analysis, which can be more easily confirmed by Eq. (1). If the phase differences due to the electric and magnetic potentials are represented by $\Delta\phi_1$ and $\Delta\phi_2$, respectively, the total $\Delta\phi$ is given by $\Delta\phi_1+\Delta\phi_2$. When an electron beam is incident to the film from the opposite side, total $\Delta\phi$ is given by $\Delta\phi_1-\Delta\phi_2$. This result presents an unusual conclusion in that a specimen appears different when looked at from upper and lower positions.

If the summation and subtraction of the two phase differences are experimentally possible, the thickness contours ($2\Delta\phi_1$) and magnetic lines of force ($2\Delta\phi_2$) can be separately observed. The subtraction of the two phases can be carried out only by overlapping the two beams to form an interference pattern, and by then drawing contour lines of the phase difference between them. For the summation, a phase-conjugate beam is used instead of one of the two beams. This conjugate beam is formed during the reconstruction stage of the holography and is the complex conjugate of the original beam in terms of amplitude (i.e., phase value sign is reversed).

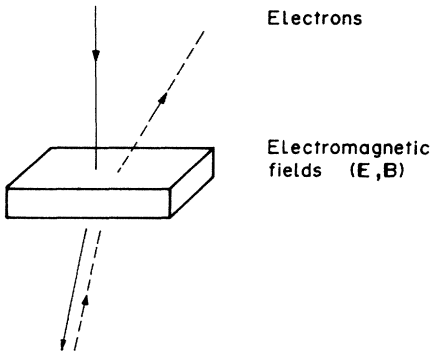

FIG. 2. Time reversal of electron trajectories in electromagnetic fields.

III. EXPERIMENTAL METHOD

A. Formation of electron hologram

An off-axis electron hologram was formed in an 80-kV field-emission electron microscope, where an electron biprism was installed between the objective and intermediate lenses. A schematic diagram of the electron-optical system is shown in Fig. 3. A specimen is located in one half of the specimen plane and its image is formed through the objective lens. A reference electron beam passes through the other half of the plane without any in-

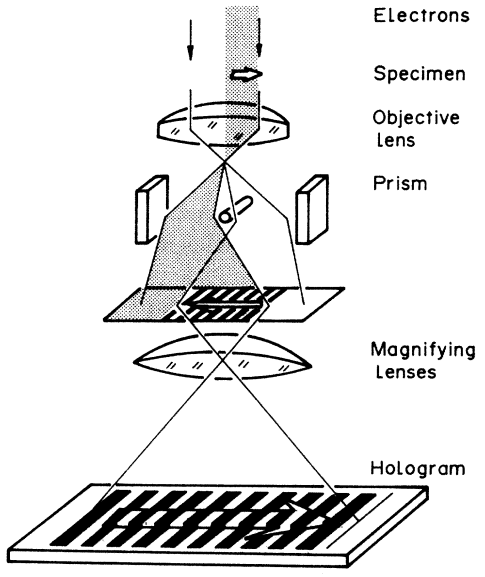

FIG. 3. Schematic diagram of electron-optical system for hologram formation.

fluence from the specimen. The two beams are overlapped using the biprism to form an interference pattern, which is further enlarged by magnifying lenses, and this pattern is recorded on film as a hologram. A pair of holograms are formed for each specimen: conventional hologram (I), and that for the reversed specimen (II). The magnification of the specimen is approximately 40 000 times.

B. Optical reconstruction system

When an electron hologram is illuminated using a collimated laser beam, the original electron wave is reconstructed by the light wave (i.e., the electron wave front is reproduced as a light wave front). Consequently, the image of the specimen is formed in three dimensions. The lateral and longitudinal image magnifications generally differ, depending on the hologram magnification and the ratio of the two wavelengths. When the magnification equals the ratio of light to electron wavelength, the two magnifications are equal, the reconstructed wave front is an undistorted replica of the original one.

A conventional interference micrograph can be obtained using the optical reconstruction system shown in Fig. 4. A collimated laser beam is split by a Mach-Zehnder-type interferometer into two beams traveling in different directions. Each beam produces a reconstructed image and its conjugate. The interference micrograph can be obtained if the reconstructed image of one beam and the other transmitted beam are adjusted to pass through the aperture for overlapping on the observation plane.

An interference micrograph can easily be formed where the phase distribution is given by the summation or subtraction of the two phase distributions. This method is described by the schematic diagram shown in Fig. 5. A pair of electron holograms of a specimen, I and II, are combined so that the two images exactly overlap. Since the specimen was viewed from the opposite direction in forming hologram II, this hologram must be turned over prior to combination. Furthermore, the carrier fringes in two holograms do not always have to coincide with each other, as illustrated in Fig. 6(a). In this figure, the two images of a pentagonal particle exactly overlap, but the directions of the carrier fringes differ between the two holograms.

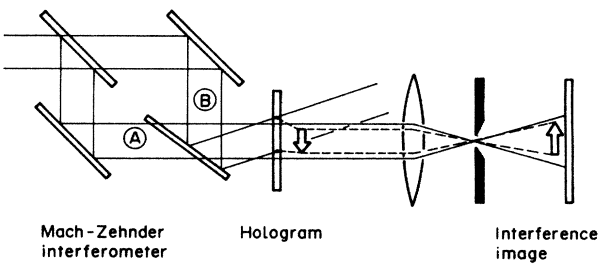

FIG. 4. Schematic diagram of optical reconstruction system for interference microscopy.

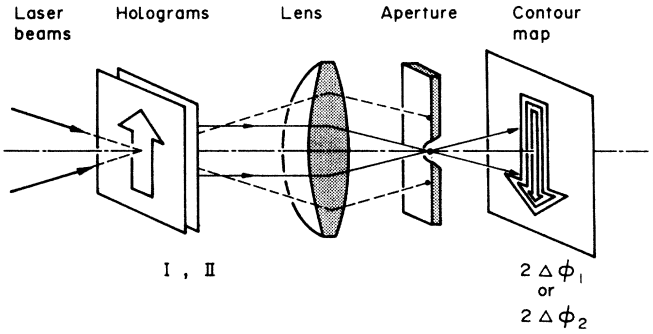

FIG. 5. Optical reconstruction system for summation and subtraction of two phase distributions.

The diffraction pattern formed on the back focal plane of the lens (aperture plane in Fig. 5) when a collimated laser beam illuminates the holograms is shown in Fig. 6(b). A pair of diffraction spots appear from hologram I, one for a reconstructed image whose phase distribution is expressed by $\Delta\phi_1+\Delta\phi_2$, and the other for its conjugate $-(\Delta\phi_1+\Delta\phi_2)$. The other pair of spots from hologram II produce a reconstructed image $\Delta\phi_1-\Delta\phi_2$ and its conjugate $-(\Delta\phi_1-\Delta\phi_2)$. Since two collimated beams illuminate a hologram, two sets of diffraction patterns such as those shown in Fig. 6(b) are produced on the back focal plane. By adjusting the incident angles of the illuminating beams, any arbitrary combination of only two beams can be selected for passing through the aperture. In this way, an interference micrograph can be formed between the two beams on the observation plane.

If a reconstructed image from hologram I $(\Delta\phi_1+\Delta\phi_2)$ overlaps with a conjugate image from hologram II $(-\Delta\phi_1+\Delta\phi_2)$, an interference micrograph is formed with phase distribution $2\Delta\phi_1$. This micrograph represents the thickness contour map of the specimen which is phase-amplified two times. Similarly, if a reconstructed image from hologram I $(\Delta\phi_1+\Delta\phi_2)$ overlaps with that from hologram II $(\Delta\phi_1-\Delta\phi_2)$, an interference micrograph is produced with phase distribution $2\Delta\phi_2$. These contour lines represent the magnetic lines of force.

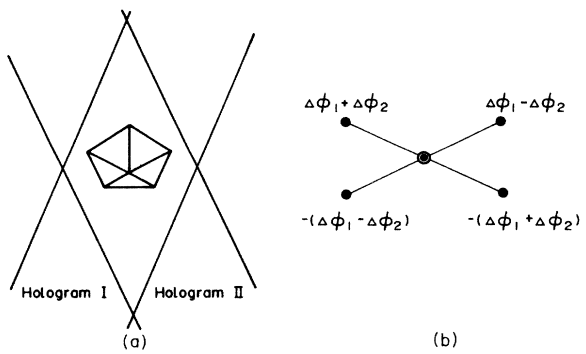

FIG. 6. Superposed two holograms. (a) Holograms. (b) Optical diffraction pattern.

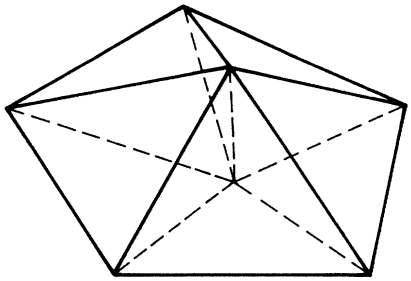

FIG. 7. Morphology of cobalt particle.

C. Specimen preparation

Cobalt fine particles were used as a specimen for the experiment. They were produced by gas evaporation in a 10-Torr atmosphere of Ar gas, and then placed on a thin carbon film. Among the several particle shapes, a pentagonal dodecahedron is selected as a specimen. This is because the magnetization in such a particle, which has a three-dimensional shape, is difficult to determine by Lorentz microscopy. The shape of such a particle is illustrated in Fig. 7. This particle consists of five regular tetrahedrons having a common edge. However, a slight opening does exist between them, so the particle is called a multiply twinned particle[14] or compound particle.[15]

IV. RESULTS AND DISCUSSIONS

Holographic interference electron microscopy was employed to determine the magnetic domain structure in cobalt fine particles which have the morphology of a pentagonal dodecahedron. The domain structure inside such a three-dimensional particle is difficult to predict,[16] since many potential choices are available. In addition, the effect of nonuniform thickness also complicates the determination from an experimental point of view.

Interference micrographs of a cobalt particle viewed from both directions were obtained as shown in Figs. 8(a) and 8(b). The contour fringes in these micrographs appear different. First, the number of contour fringes observed differs by approximately two times. Second, the fringe spacing widens more at the particle center than at the periphery in micrograph (b) while it narrows in micrograph (a). From these differences, it can be concluded that a magnetic contribution exists which is comparable to the thickness one. Without these differences, the same micrograph should theoretically be obtained.

The summation and subtraction of these two phase distributions were carried out in the optical system of Fig. 5, and the resultant interference micrographs are shown in Fig. 9. Micrograph (a), which represents $2\Delta\phi_1$, shows the thickness contour map of the particle phase-amplified two times. The contour lines in micrograph (b) with $2\Delta\phi_2$ represent the magnetic lines of force. From micrograph

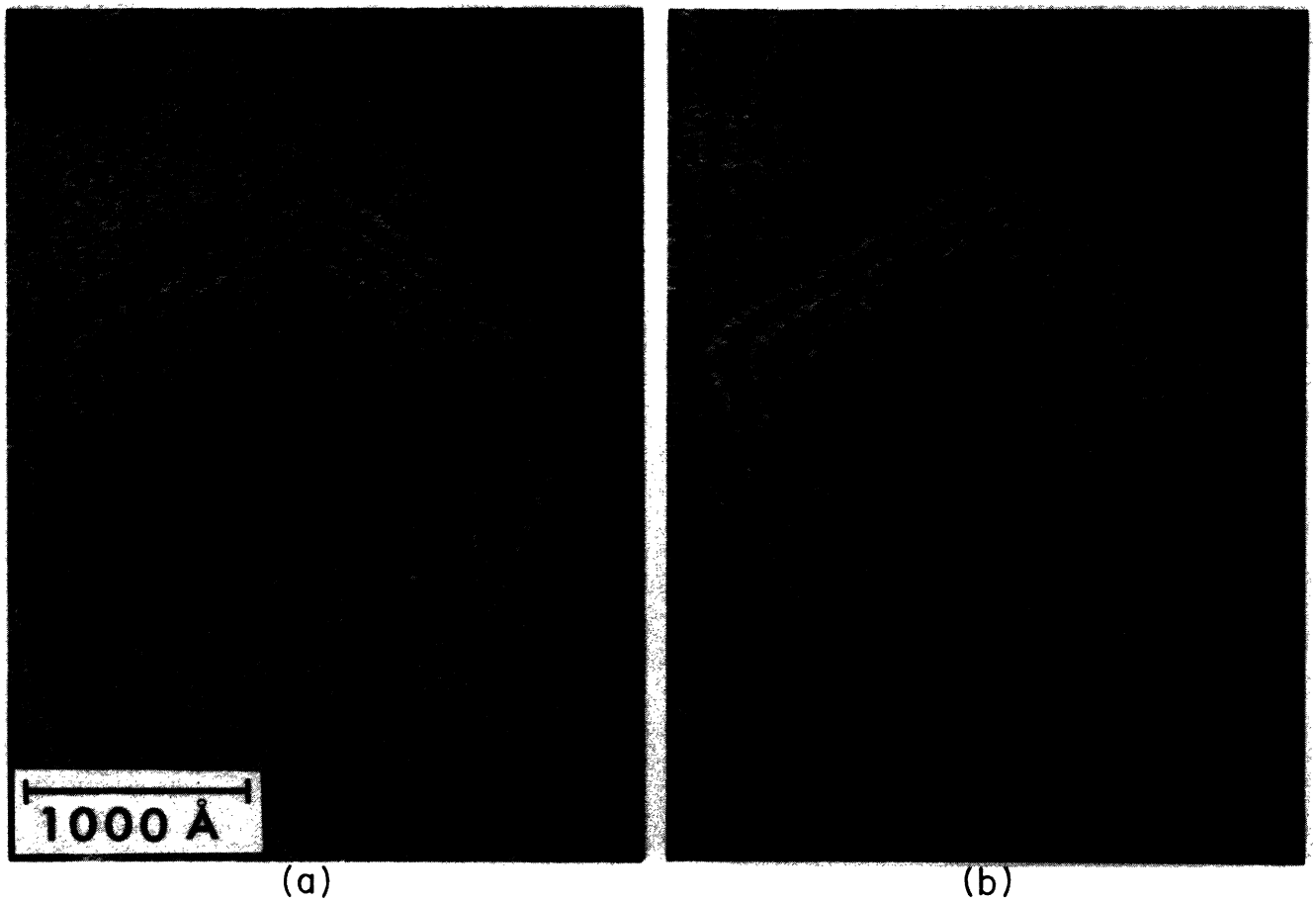

FIG. 8. Interference micrographs of a cobalt particle viewed from two opposite directions. (a) $\Delta\phi_1+\Delta\phi_2$. (b) $\Delta\phi_1-\Delta\phi_2$.

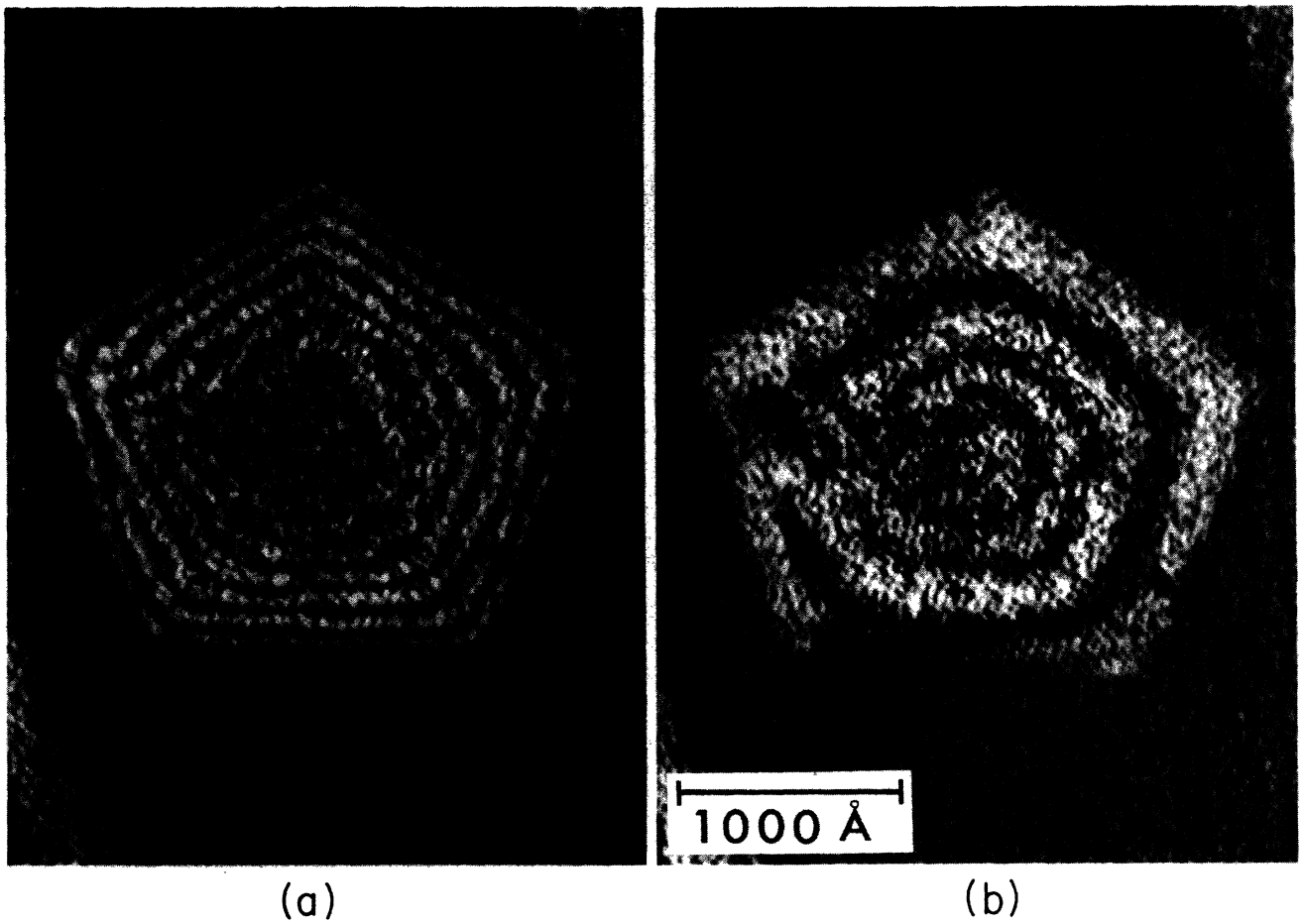

FIG. 9. Interference micrographs of a cobalt particle. (a) Thickness contour lines ($2\Delta\phi_1$). (b) Magnetic lines of force ($2\Delta\phi_2$).

(b), it can be concluded that the particle has an internal rotational magnetization, as schematically shown in Fig. 10. Arii *et al.*[17] previously reported that two kinds of different Lorentz micrographs exist for particles which are similar in shape and size. This finding suggests the existence of rotational magnetization.

From the thickness contour map, it is found that the fringe spacing is equal, which is consistent with the particle morphology illustrated in Fig. 7. A disturbance in the contour fringes is observed in the left part of the particle in all of the interference micrographs. This disturbance may be due to the crystalline imperfection at the opening between the regular tetrahedrons. At that point, incident electron beams undergo a slight phase shift due to the different Bragg-reflection condition.

Since the internal magnetization of the particle was determined to be rotational, contour maps shown in Fig. 8 can also be explained by the calculation. Calculated results assuming the inner potential $V_0 = 30$ V and magnetization $M = 1450$ Oe are shown in Fig. 11. Contour map (a) ($\Delta\phi_1 + \Delta\phi_2$) corresponds to a case where the rotational

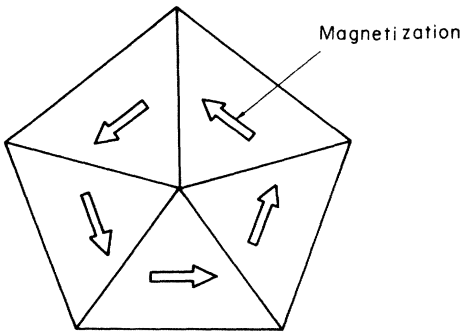

FIG. 10. Rotational magnetization in cobalt particle.

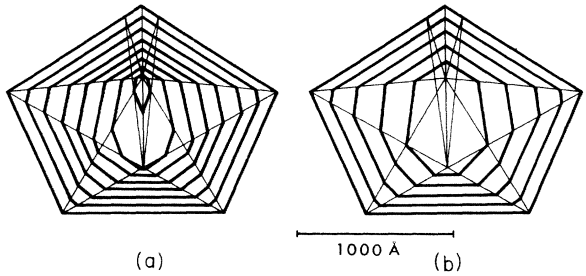

FIG. 11. Calculated interference micrographs. (a) $\Delta\phi_1 + \Delta\phi_2$. (b) $\Delta\phi_1 - \Delta\phi_2$.

magnetization direction is counterclockwise when the particle is viewed from the direction of the incident electron beam. Contour map (b) ($\Delta\phi_1 - \Delta\phi_2$), on the other hand, corresponds to the incidence of an electron beam from the opposite direction. The interference micrographs of Fig. 8 can be adequately explained from the calculated results: The spacing of the contour fringes widens more from the periphery to the center in Figs. 8(b) and 11(b), and becomes narrow in Figs. 8(a) and 11(a).

V. CONCLUSION

A new method using electron holography has been established to circumvent the problem of inseparability between electric and magnetic effects in conventional interference electron microscopy. In this method, two holograms, a conventional one and that for a reversed specimen, are first formed for a single specimen. Then the summation and subtraction of the two phase distributions are carried out during the optical reconstruction stage to form two interference micrographs. These micrographs give phase distributions which are purely electric and magnetic.

This method was then applied practically for determining the magnetization distribution in a three-dimensional ferromagnetic particle. In such a specimen, the thickness change produces an additional phase difference, which has made it impossible to interpret by conventional interference microscopy. However, it could be determined by the new method that a cobalt fine particle with the shape of a pentagonal dodecahedron has a rotational magnetization around the axis which is determined by the common edge of five regular tetrahedrons forming the particle.

---

[1]G. F. Missiroli, G. Pozzi, and V. Valdré, J. Phys. E **14**, 649 (1981).

[2]K.-J. Hanszen, *Advances in Electronics and Electron Physics*, edited by C. Marton (Academic, New York, 1982), Vol. 59, p. 1.

[3]A. Tonomura, J. Electron Microsc. **33**, 101 (1984).

[4]A. Tonomura, T. Matsuda, J. Endo, H. Todokoro, and T. Komoda, J. Electron Microsc. **28**, 1 (1979).

[5]A. Tonomura, J. Endo, and T. Matsuda, Optik (Stuttgart) **53**, 143 (1979).

[6]A. Tonomura, T. Matsuda, J. Endo, T. Arii, and K. Mihama, Phys. Rev. Lett. **44**, 1430 (1980).

[7]A. Tonomura, T. Matsuda, H. Tanabe, N. Osakabe, J. Endo, A. Fukuhara, K. Shinagawa, and H. Fujiwara, Phys. Rev. B **25**, 6799 (1982).

[8]This restriction on a specimen is also imposed on Lorentz microscopy, since thickness variations produce not only a phase shift of an electron beam but also its deflection.

[9]W. Ehrenberg and R. E. Siday, Proc. Phys. Soc. London, Sect. B **62**, 8 (1949).

[10]If Bragg reflections are excited in a crystalline specimen, periodic potential V_h has to be taken into consideration. Such diffraction effects were actually observed: K. Yada, K. Shibata, and T. Hibi, J. Electron Microsc. **22**, 223 (1973); K.-J. Hanszen, Phys. Bl. **39**, 283 (1983).

[11]In addition to the method described in this paper, the following methods can also be considered for the present purpose: One is to utilize an additional micrograph of a specimen at a temperature higher than the Curie one, which represents a thickness contour map. Another is to obtain two interference micrographs with electron beams of different accelerating voltages, which have different ratios of electric and magnetic contributions.

[12]The time-reversal operation was used to prove the magnetic nature of the ripple constant in a Lorentz micrograph: H. Boersch and H. Raith, Naturwissenschaften **20**, 574 (1959). For the related theoretical discussions, see D. Wohlleben, in *Electron Microscopy in Material Science*, edited by U. Valdrè (Academic, New York, 1971), p. 712.

[13]If magnetic fields are produced from the movement of electric charges, or from spin, the field directions are reversed on time reversal. Therefore, the symmetry for time reversal is not broken.

[14]S. Ino, J. Phys. Soc. Jpn. **21**, 346 (1966).

[15]K. Mihama and Y. Yasuda, J. Phys. Soc. Jpn. **21**, 1161 (1966).

[16]A similar problem was also investigated for determining the magnetic domain structure of three-dimensional fine iron particles: T. Arii, K. Mihama, T. Matsuda, and A. Tonomura, J. Electron Microsc. **30**, 121 (1981).

[17]T. Arii, S. Yatsuya, N. Wada, and K. Mihama, in *Proceedings of the Fifth International Conference on High Voltage Electron Microscopy, Kyoto, 1977*, edited by T. Imura and H. Hashimoto (Japanese Society of Electron Microscopy, Tokyo, 1977), p. 203.

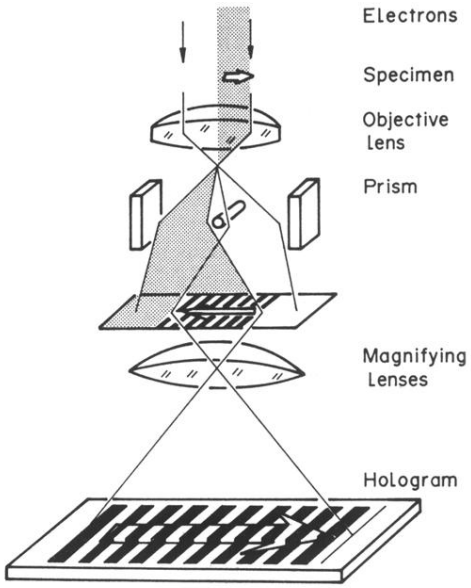

FIG. 3. Schematic diagram of electron-optical system for hologram formation.

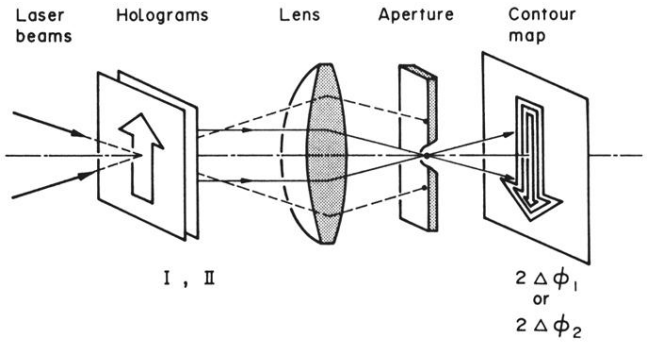

FIG. 5. Optical reconstruction system for summation and subtraction of two phase distributions.

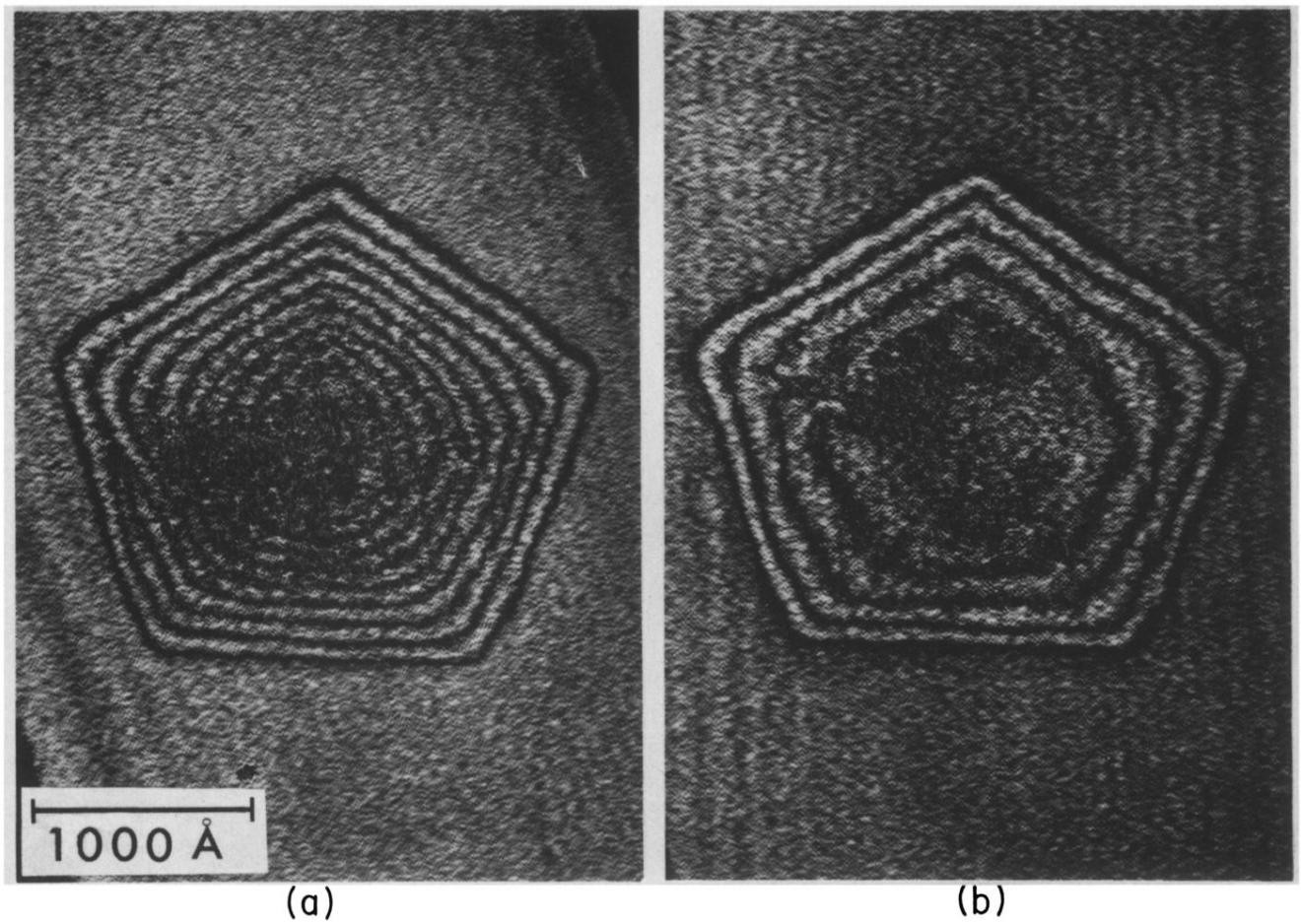

FIG. 8. Interference micrographs of a cobalt particle viewed from two opposite directions. (a) $\Delta\phi_1+\Delta\phi_2$. (b) $\Delta\phi_1-\Delta\phi_2$.

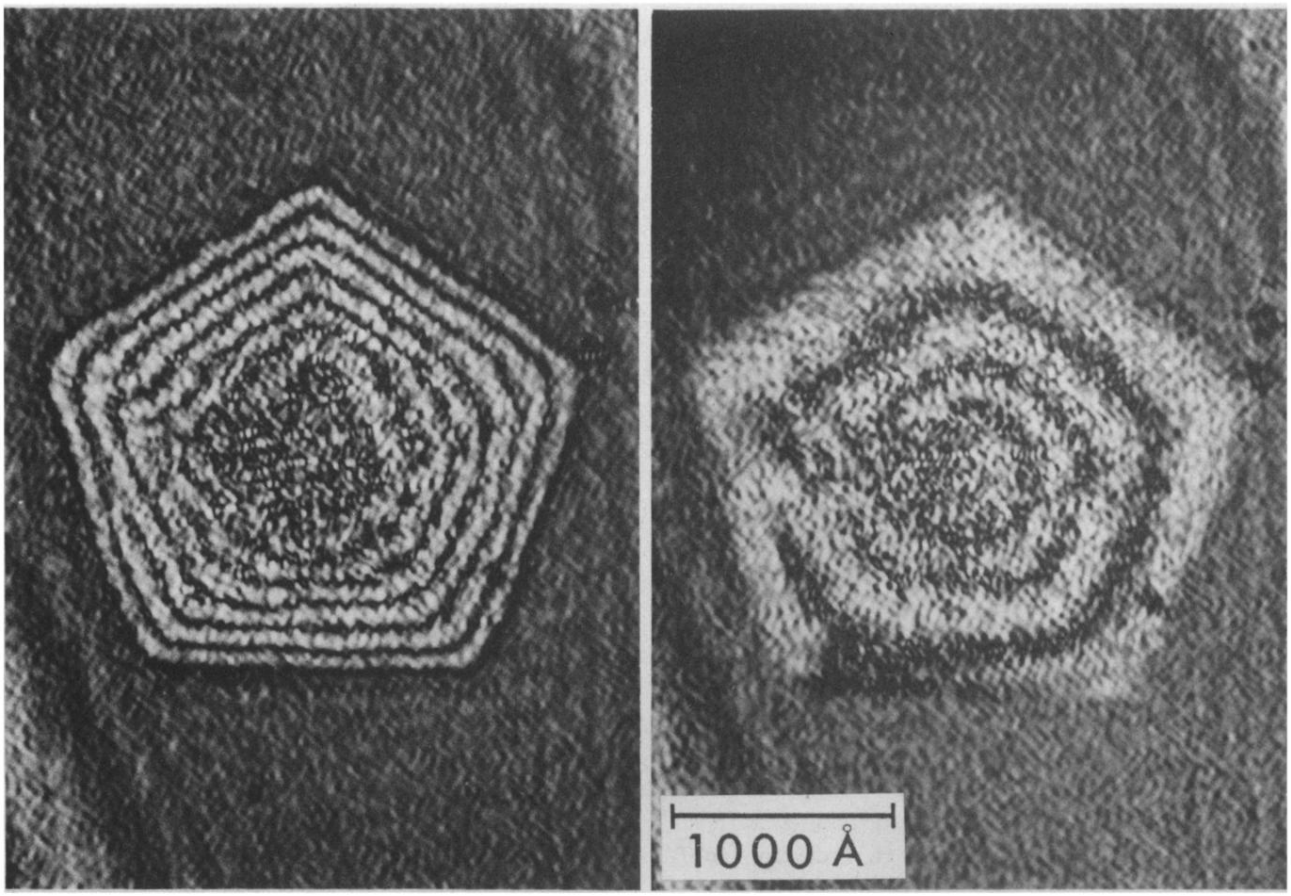

FIG. 9. Interference micrographs of a cobalt particle. (a) Thickness contour lines ($2\Delta\phi_1$). (b) Magnetic lines of force ($2\Delta\phi_2$).